# Strategies for computing the scalar self-force on a Schwarzschild background

Steven Dorsher

Louisiana State University

September 26, 2017

# Gravitational Waves

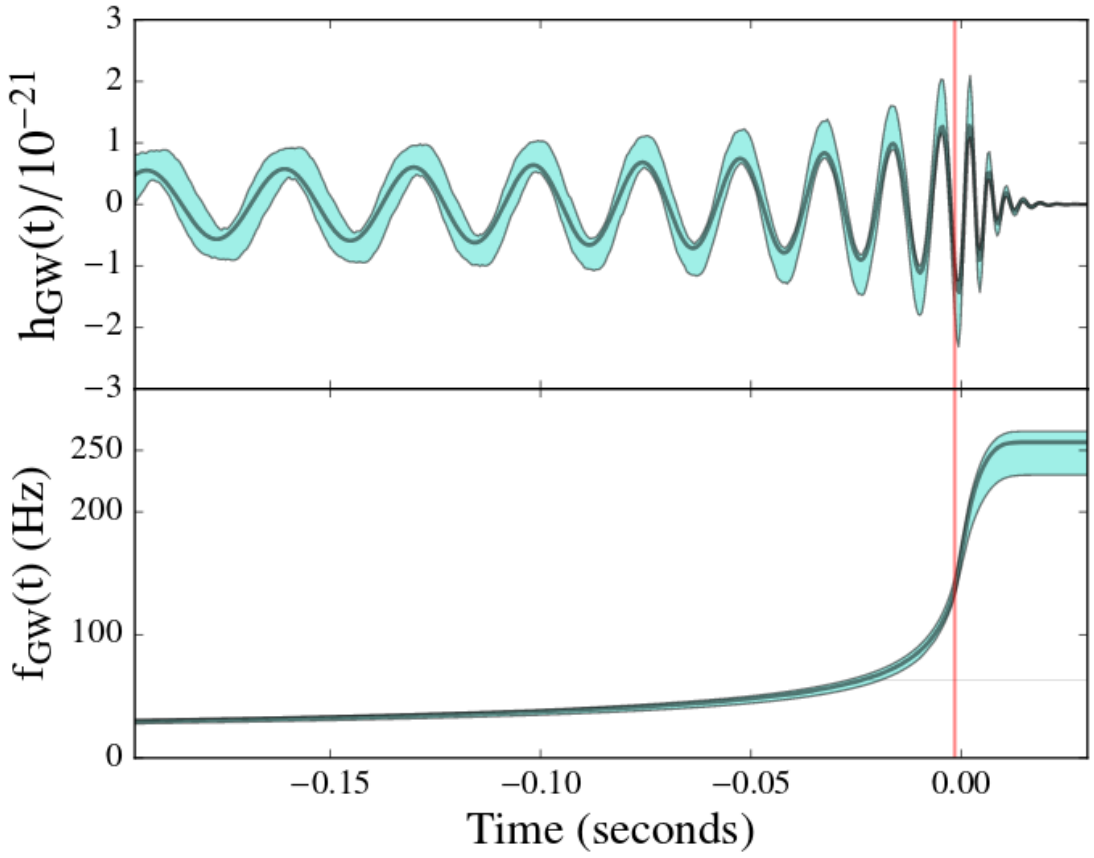


Figure: LIGO detection, September 14, 2015. General relativity was tested by comparing inpsiral with merger/ringdown phases.

# Extreme Mass Ratio Inspirals

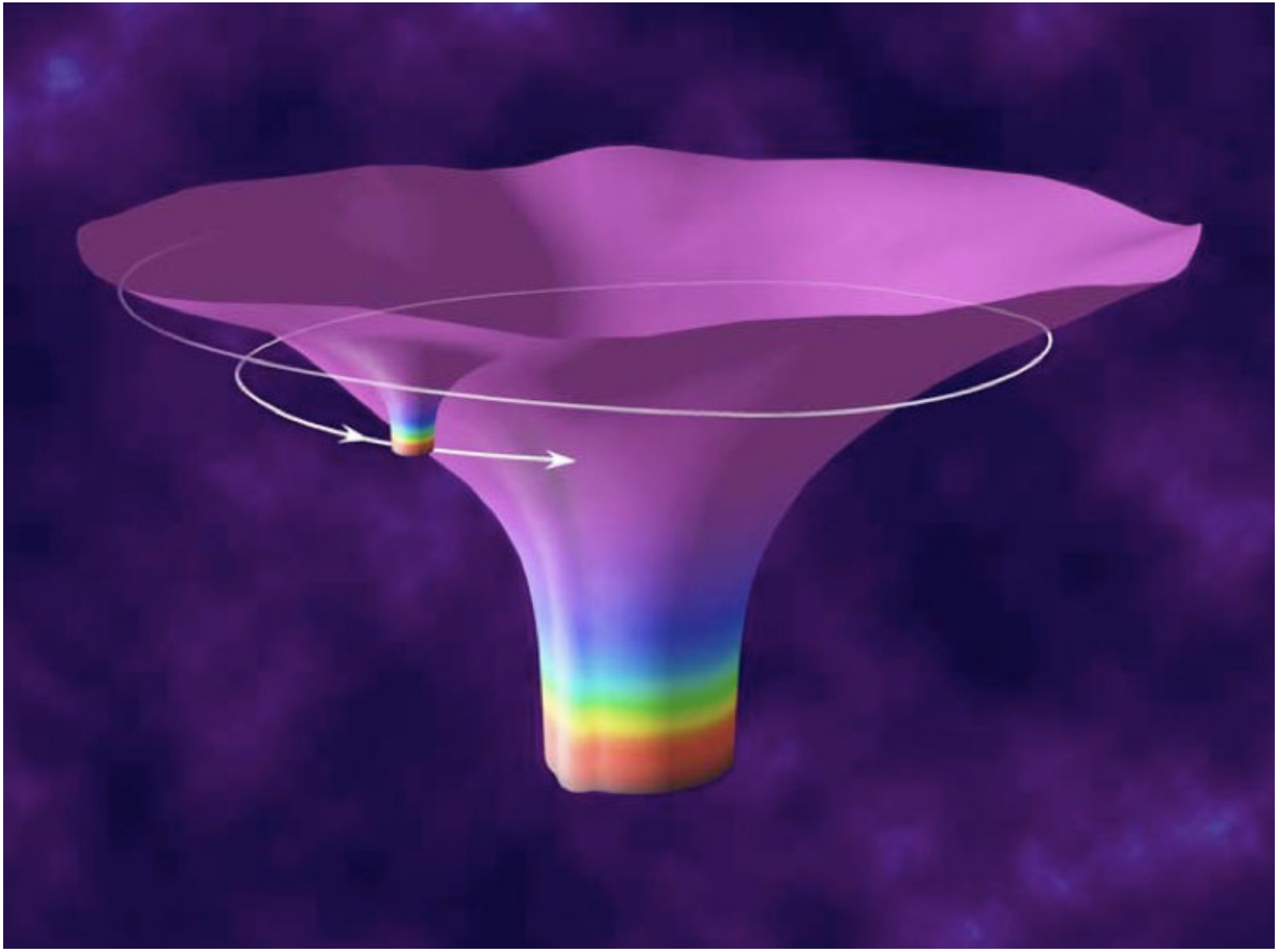

# Laser Interferometer Space Antenna

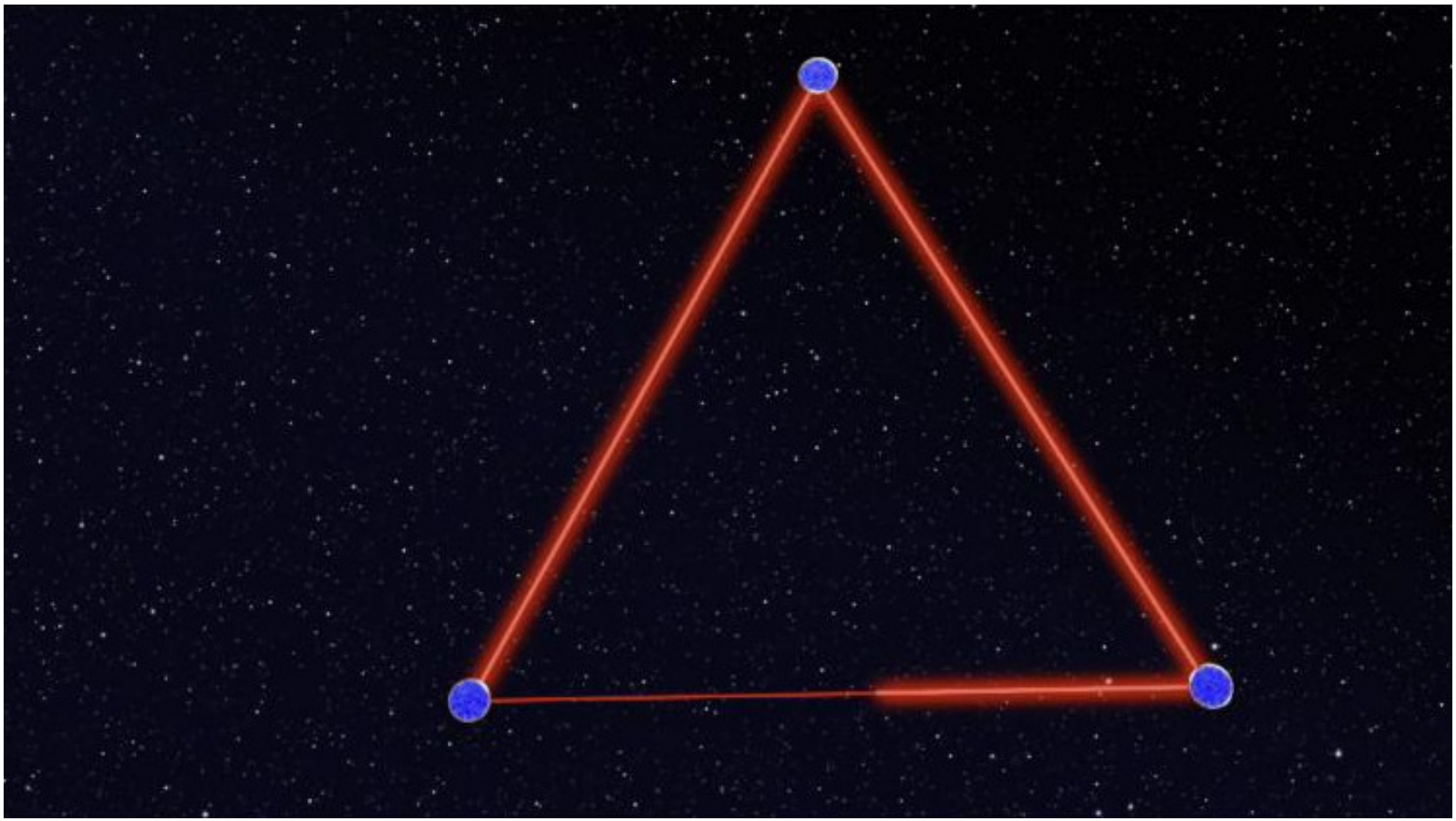

Figure: Laser Interferometer Space Antenna, which will operate around launches in early 2030's, ESA-NASA partnership, will detect EMRI's

# Toward LISA EMRI templates

- Generating LISA EMRI templates require resolving $10^6$ orbits with precision on the order of $\delta P/P \sim 10^{-6}$ *Danzmann, Karsten. LISA: A proposal in response to the ESA call for L3 mission concepts (2017)*
- For EMRI's, the self-force approximation is used in the limit where the mass ratio is large ($10^4$ to $10^6$)
- Nearly equal mass numerical relativity uses spacetimes with initial conditions smoothly matched between the two blackholes, consistently evolved
- EMRI's have an orbital evolution timescale that scales as $M/\mu$, and a period that scales as $M$. These two widely different timescales necessitate a different numerical approach than numerical relativity.
- Self-force is a perturbative approximation in either the distance from the small black hole or the mass ratio.

# Self-force in a classical atom

- Consider a classical atom without quantization (not even a Bohr atom)
- The electron orbits the nucleus
- It radiates energy because it is accelerated
- Because it radiates energy, it becomes more tightly bound
- The electron spirals inward
- The self-force of the particle interacting with its own field causes this

# Self-force in general relativity

- In general relativity, test particles move along geodesics
- A compact object is not a test particle
- Motion $\rightarrow$ radiation $\rightarrow$ energy and angular momentum loss $\rightarrow$ inspiral
- The self-force is a finite-mass particle's interaction with its own field that causes the inspiral
- Applies to scalar, electromagnetic, and tensor fields on a gravitational background
- We use perturbative expansion in terms of powers of radius from small black hole– perturbations of the orbit

# Approximations and Goals

The long term goal for the field is to generate extremely precise EMRI gravitational wave templates for LISA.
Approximations:

- Scalar rather than tensor waves ($\Psi$ rather than $h_{\mu\nu}$)
- Non-rotating black holes: Schwarzschild spacetime
- Self-force causes a particle to inspiral as it emits radiation
- We use the Detweiler-Whiting effective source as implemented by Barry Wardell
- In our self-consistent evolution, our self-force naturally takes into account the past history of the particle
- Niels Warburton assumes: the particle has been on the same geodesic for all time when he calculates the self-force

Our goal is to implement a highly accurate self-consistent evolution and do a comparison study with Niels Warburton.

# Schwarzschild spacetime without a source

- Wave equation: $\Box\Psi = \frac{1}{\sqrt{-g}}\partial_\mu\left(g^{\mu\nu}(\partial_\nu\Psi)\sqrt{-g}\right) = 0$
- Multipole moment decomposition to account for angular dependence
- Quasinormal mode (QNM) ringing
  - higher frequencies and faster decay for higher $l$
  - due to interactions near peak of potential
- Power law tails
  - go as $t^{-(2l+3)}$
  - follow the QNM
  - due to scattering off spacetime far from the peak of the potential

# Quasinormal modes

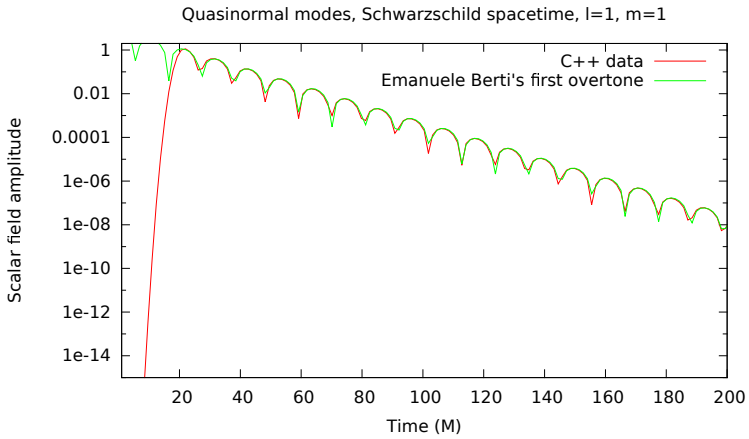


(a) $l = 1$

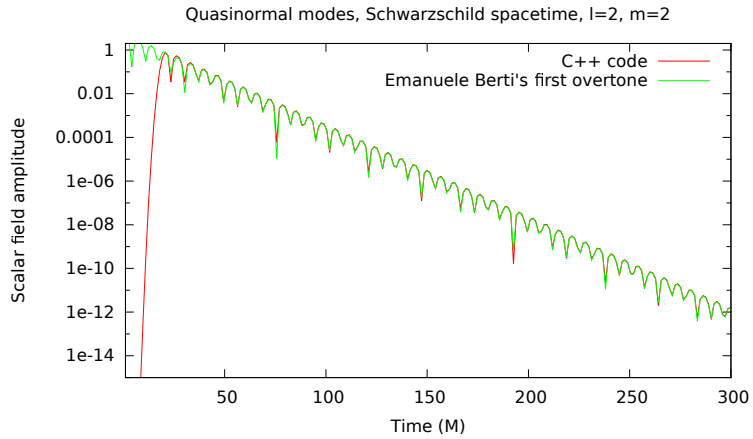


(b) $l = 2$

Figure: $l = 2$ has a higher frequency and a faster decay rate than $l = 1$

# Power law tails

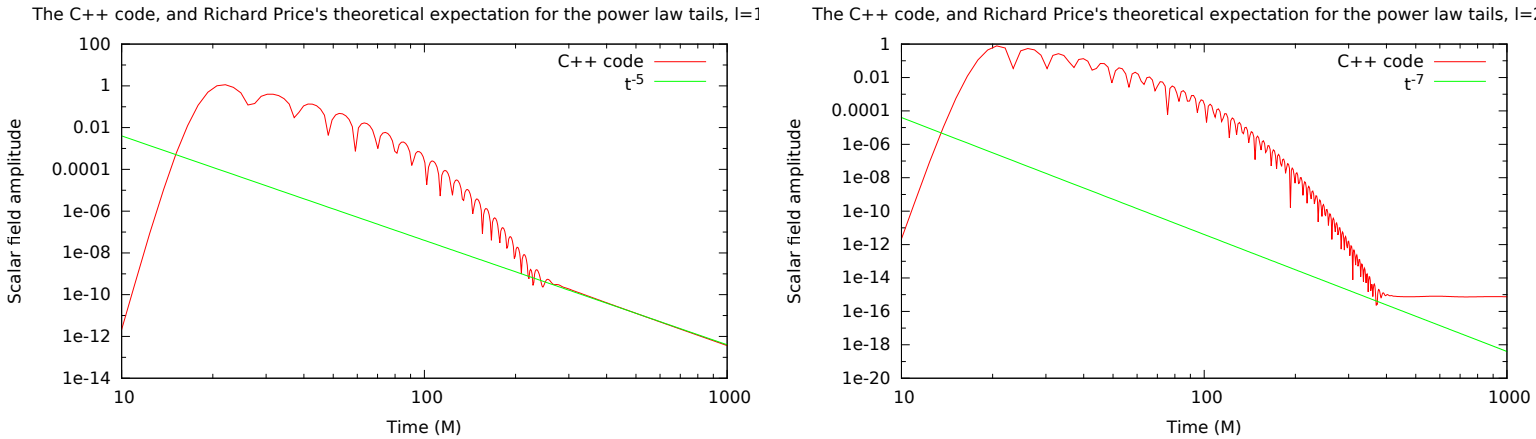


(a) $l = 1$ (b) $l = 2$

Figure: $l = 1$ decays as $t^-−5$ as expected; however, $l = 2$ has no power law tail due to truncation error

# Scalar charge on a circular orbit with an effective source

- Self-force causes the particle to emit radiation and inspiral. An artifical force holds it on a circular orbit.
- Regularize field: $\Psi^R = \Psi^{ret} - \Psi^S$
- Detweiler-Whiting singular field: *Steven Detweiler, Bernard F. Whiting (2002). Phys. Rev. D 67, 024025*
- $\Box\Psi^R = S_{eff} = \Box\Psi^{ret} - \Box(W\tilde{\Psi}^S) = -q4\pi \int \delta_4(x, z(\tau'))d\tau'$
- Wave equation for retarded field has delta function effective source proportional to charge in the scalar case.
- In tensor case for gravitational field, perturbative expansion in terms of powers of radius: *Anna Heffernan, Adrian Ottewill, Barry Wardell (2012). Phys. Rev. D 86, 104023*
- I have ported this from Fortran to C++ with partially redesigned structure. I have succeeded in reproducing the results to roundoff error precision.

# Circular orbit roundoff error comparison between languages

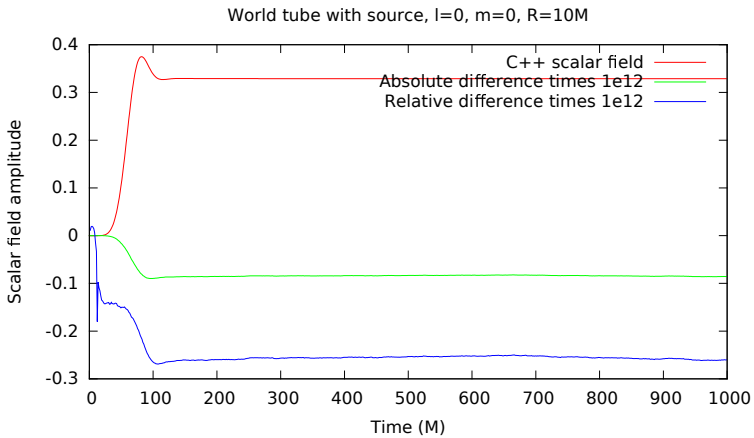


(a) l=0

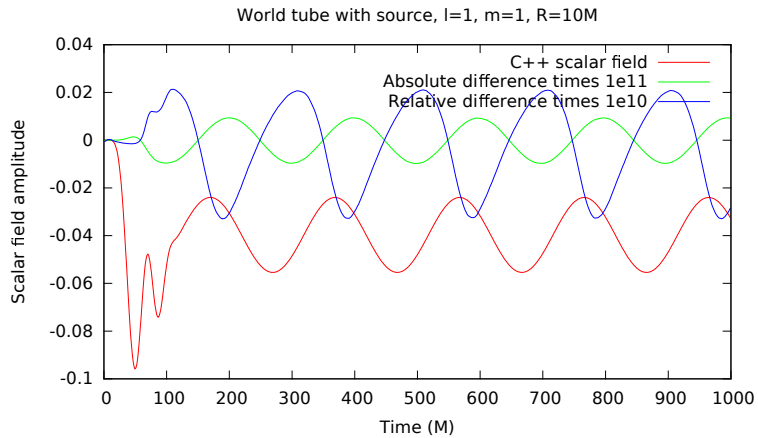


(b) l=1

Figure: Relative and absolute errors are at the roundoff level– $10^{-10}$ to $10^{-12}$. Oscillations do not appear in the $l = 0$ mode but appear with the orbital period in the $l = 1$ mode.

# Eccentric orbits using Peter Diener's simulation

- $\chi$, $\phi \rightarrow$ precession
- The orbit is artifically held on a geodesic to counteract the self-force generating the scalar waves
- $p$, $e$ held fixed, monotonically evolving $\chi$, $\phi$
- $r_{periastron} = \frac{pM}{1+e}$, $r_{apastron} = \frac{pM}{1-e}$
- Radial self-force: $F_r = q\partial_r \Psi^R$
- Warburton initial conditions: particle has been on the same geodesic for all time
- Diener initial conditions: field starts at zero with particle at aphelion

# Precession of the eccentric orbit

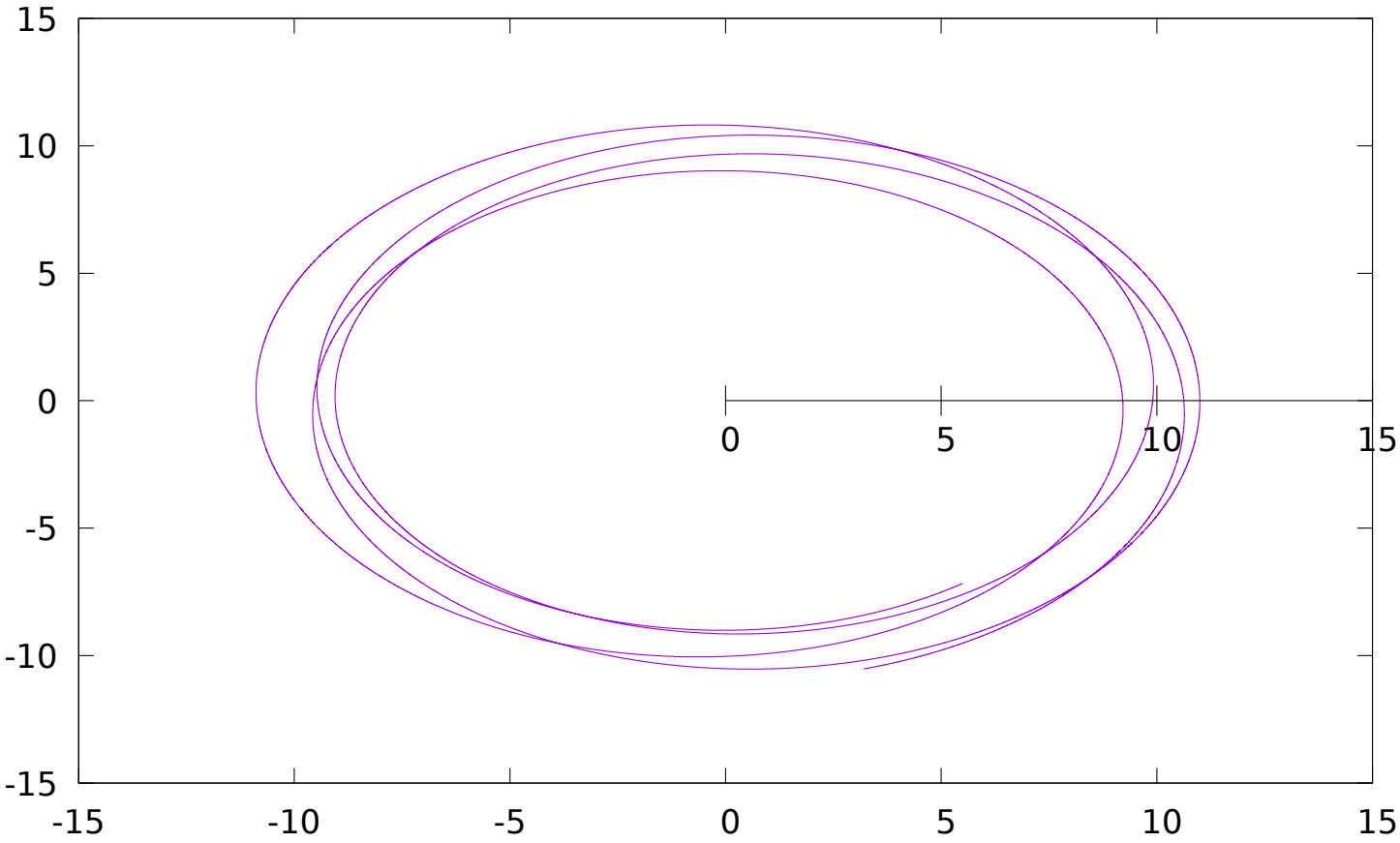


Figure: Precession of the eccentric orbit. $p = 9.9$, $e = 0.0$.

# Evolution of the radial self-force for different initial conditions

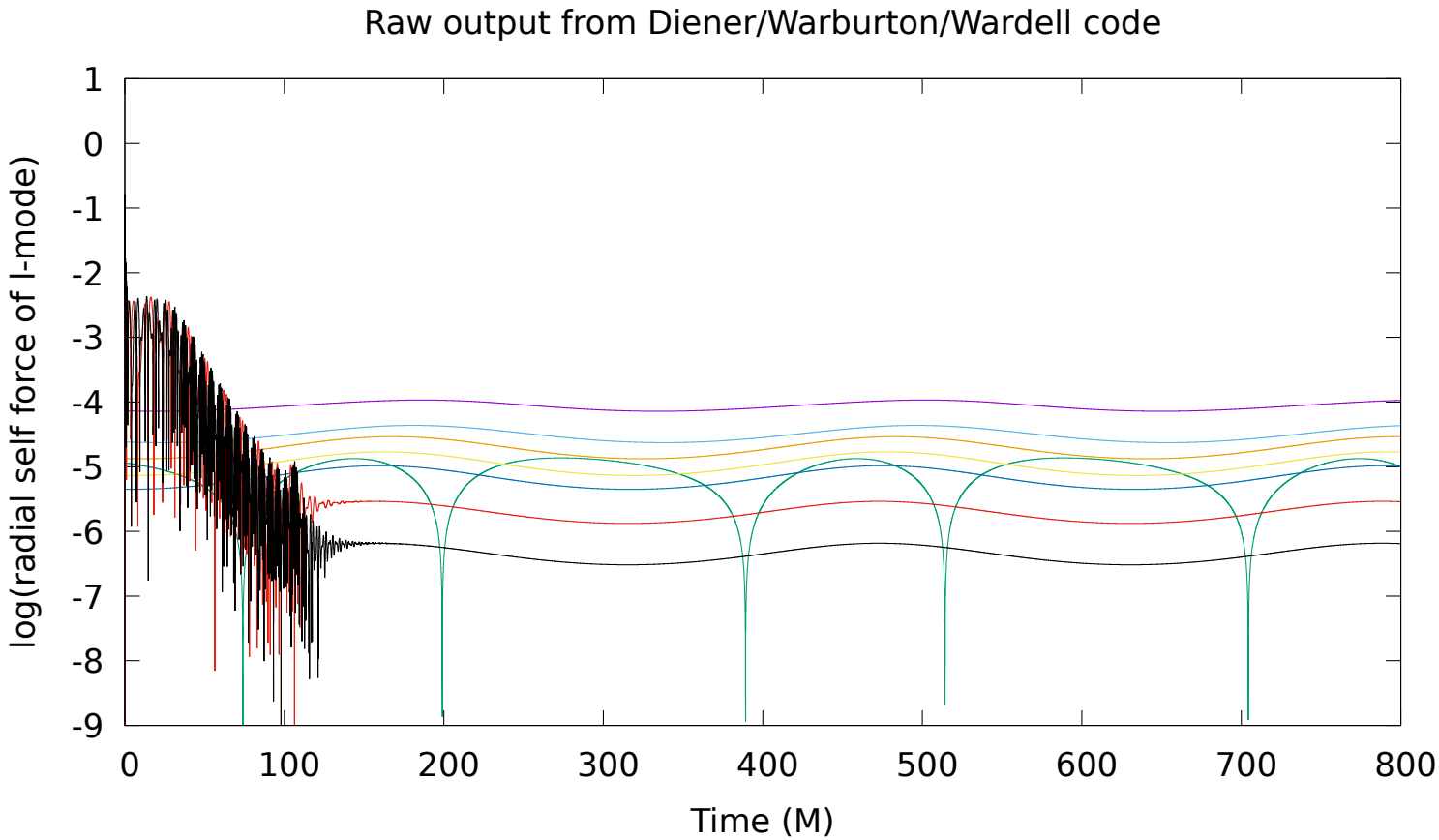


Figure: Modes zero through seven are shown. Zero through five have smooth starts. Six and seven have transients.

# Addressing instabilities and error

- I characterized the error in the eccentric evolutions due to
  - Neglecting the first order Richardson extrapolation
  - Choice of start and end modes in mode sum fit
  - Choice of number of terms in mode sum fit
  - Selection of weights associated with mode sum fit
- Concluded the first three errors were comparable and at the $10^{-4}$ level and the fourth was negligible. This is a one order of magnitude improvement over a previous study that made use of circular orbits instead of eccentric orbits. *Ian Vega and Steven Detweiler (2008). Phys Rev D. 77, 084008.*

# The first order Richardson extrapolation

- Discontinuous Galerkin: ODE solver with errors that scale as $h^{n+1}$
- Truncation error is skewed entirely to one side when measured using $L_0$ or $L_2$ error
- Convergent code approaches an asymptote
- Assume $F_r(n, l) = F_{inf}(l) + c(l)\exp(-\alpha n)$
- Use three different DG orders arranged in steps of four to obtain an extrapolation to $F_{inf}$ from some starting order

# Well-converging data

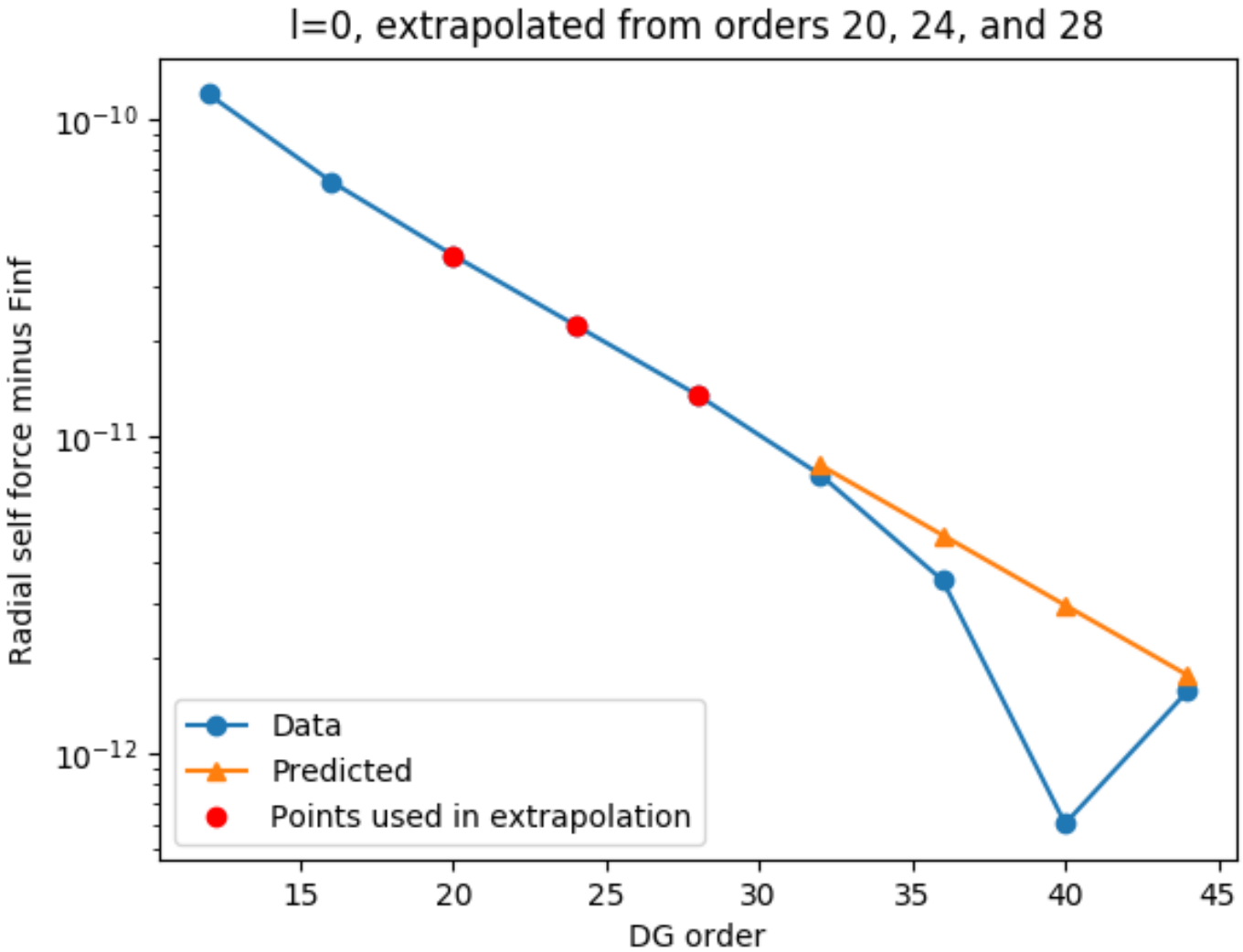


Figure: l=0 at t=370. This data converges very cleanly until it hits roundoff noise at high DG orders.

# Error due to neglecting the first order Richardson Extrapolation

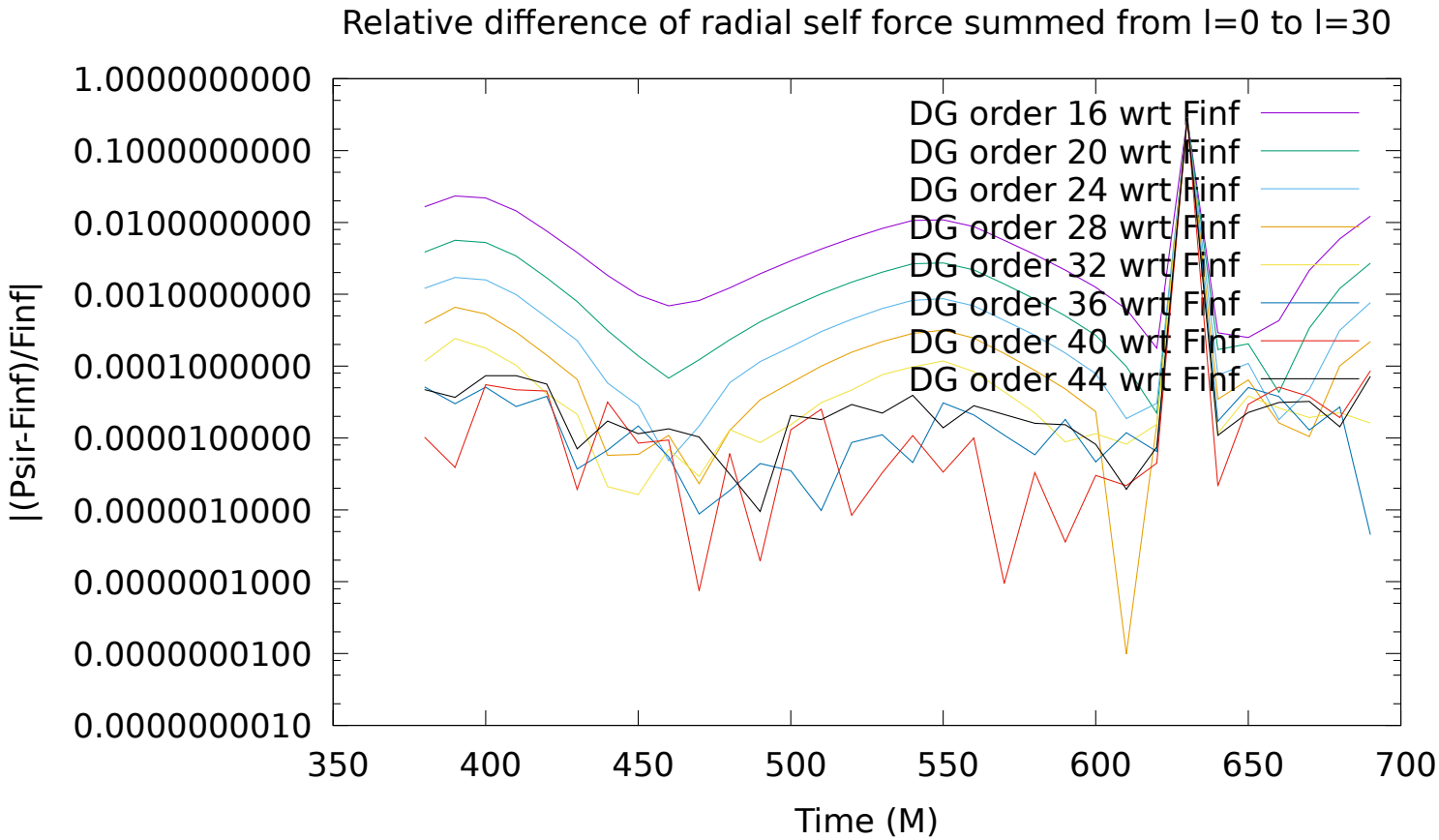


Figure: Relative error between DG starting orders and $F_{inf}$ vs time. For DG order 36 where roundoff error sets in, the error is about $10^{-4}$.

# The l-mode sum and fit

$$F_r(l,t) = \frac{A(t)}{(2l-1)(21+3)} + \frac{B(t)}{(2l-3)(2l-1)(2l+3)(2l+5)} + \frac{C(t)}{(2l-5)(2l-3)(2l-1)(2l+3)(2l+5)(2l+7)} + \cdots \quad (1)$$

*Anna Heffernan, Adrian Ottewill, Barry Wardell (2012). Phys. Rev. D 86, 104023*

- Fit from $l_{min}$ to $l_{max}$.
- Sum numerically from zero to $l_{max}$ then use fit coefficients to analytically sum to $l = \infty$

# l-mode fit

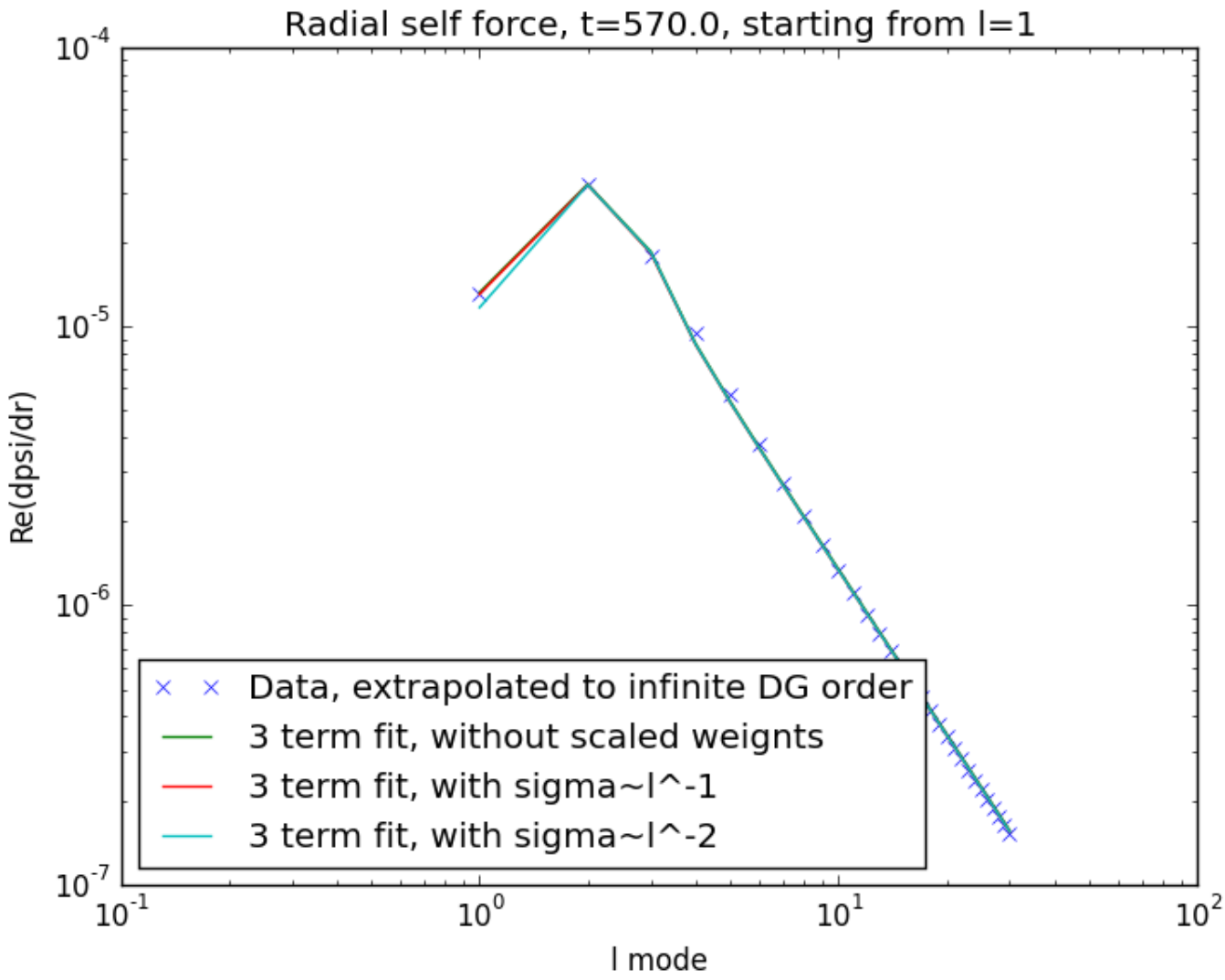


Figure: l-mode versus $F_{inf}$.

# Smooth evolution of total radial self-force

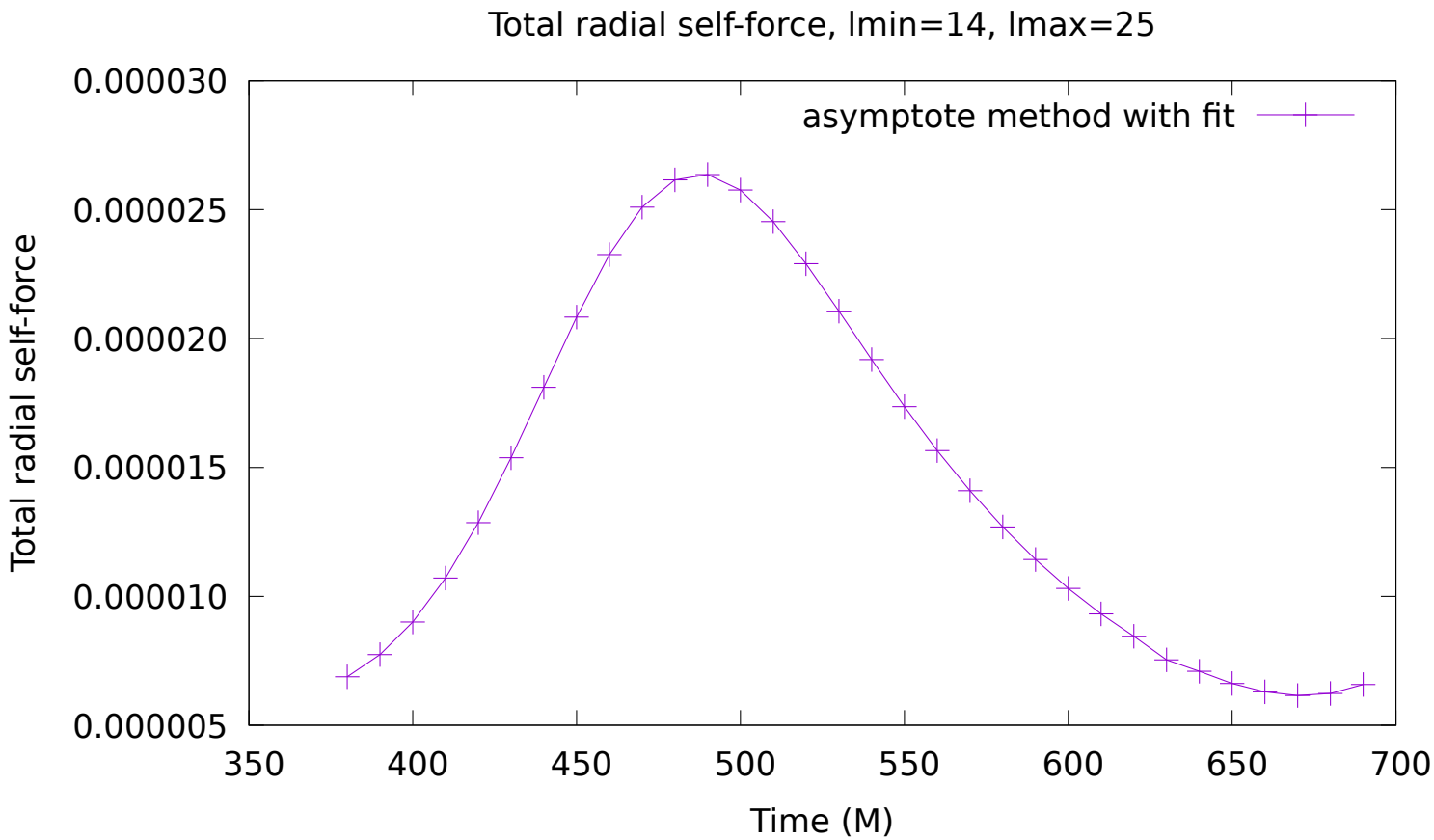


Figure: Total radial self-force including sum to $l = \infty$ over time

# Summary of l-mode fit results

- The best $l_{min} = 14$ and $l_{max}$=25. The relative error in these choice of values is $10^{-4}$.
- The relative error due to the number of terms used in the fit is $10^{-4}$.
- The error due to the use of weights in fitting is insignificant.

# Comparison study of self-consistent evolution to geodesic evolution

- Self-consistent evolution accounts for the interaction of the particle with the field it has generated in the past naturally since it is evolved in the time domain
  - Uses the Detweiler-Whiting singular field
  - The particle position evolves according to the geodesic equation with an acceleration on the right hand side
  - The mass of the particle also evolves according to the work being done on it
- Geodesic evolution uses an self-force that assumes the particle has been evolving on the same geodesic for all time
  - Self-force can be efficiently calculated in the frequency domain due to periodicity
  - Frequency domain component is good for initial conditions without transients
  - Evolves in the time domain after generating the self-force in the frequency domain
  - Cannot handle effects where the timescale of the orbital evolution is short compared to the period

# Long term goals

- Goal is to compare Diener's self-consistent code using Warburton's initial conditions and Wardell's effective source to Warburton's geodesic evolutions using frequency domain self force.
- I will run code, analyze physics, and debug, as necessary.
- In particular, some instabilities in the self-consistent evolutions need to be addressed before a publication will be possible. I will help look for a solution to those instabilities.
- Timescale: highly variable. 2-3 years potentially?

# Extra slides

# Flat space evolution

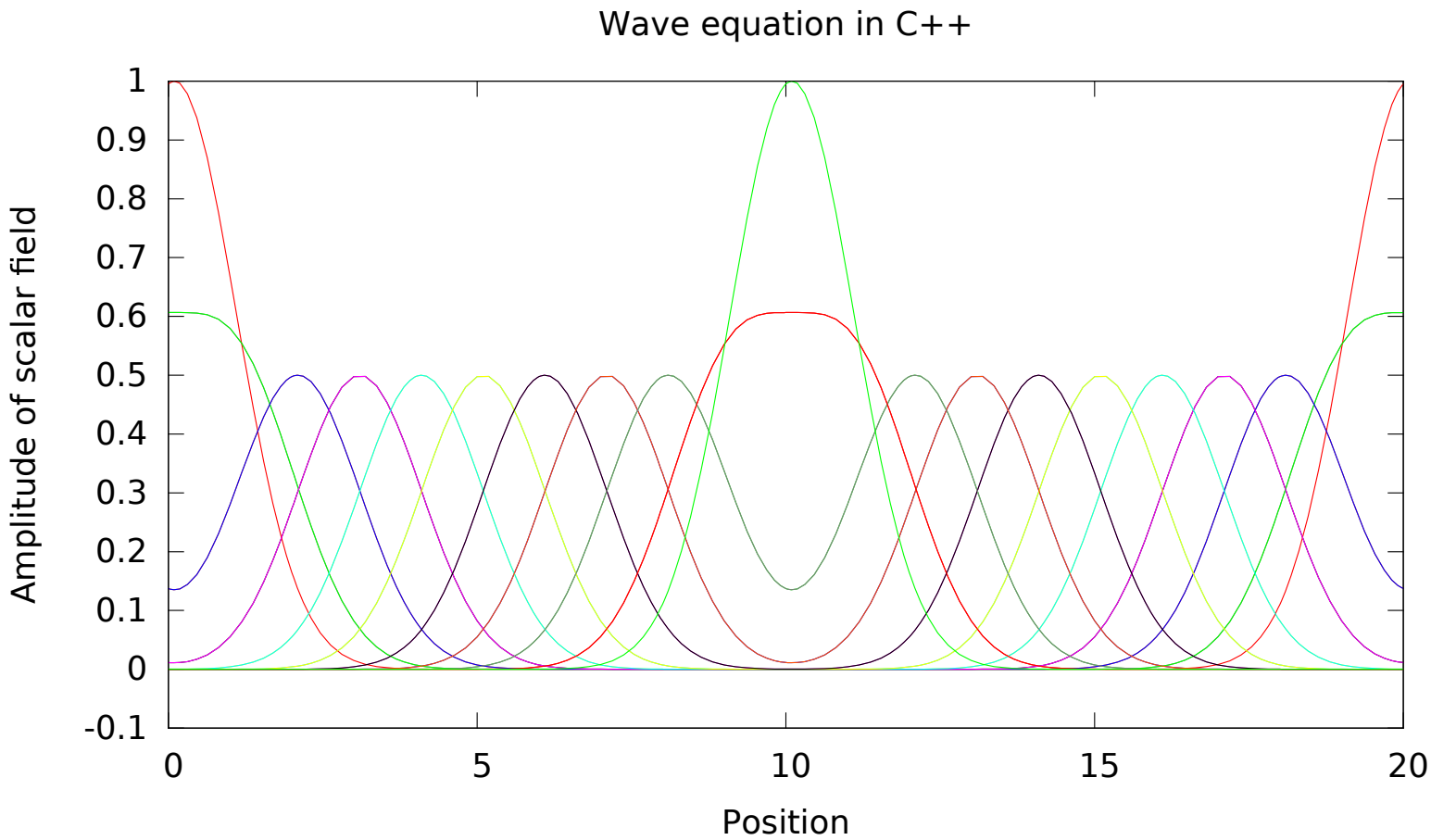


Figure: Gaussian initial conditions, flat spacetime

# Flat spacetime error convergence

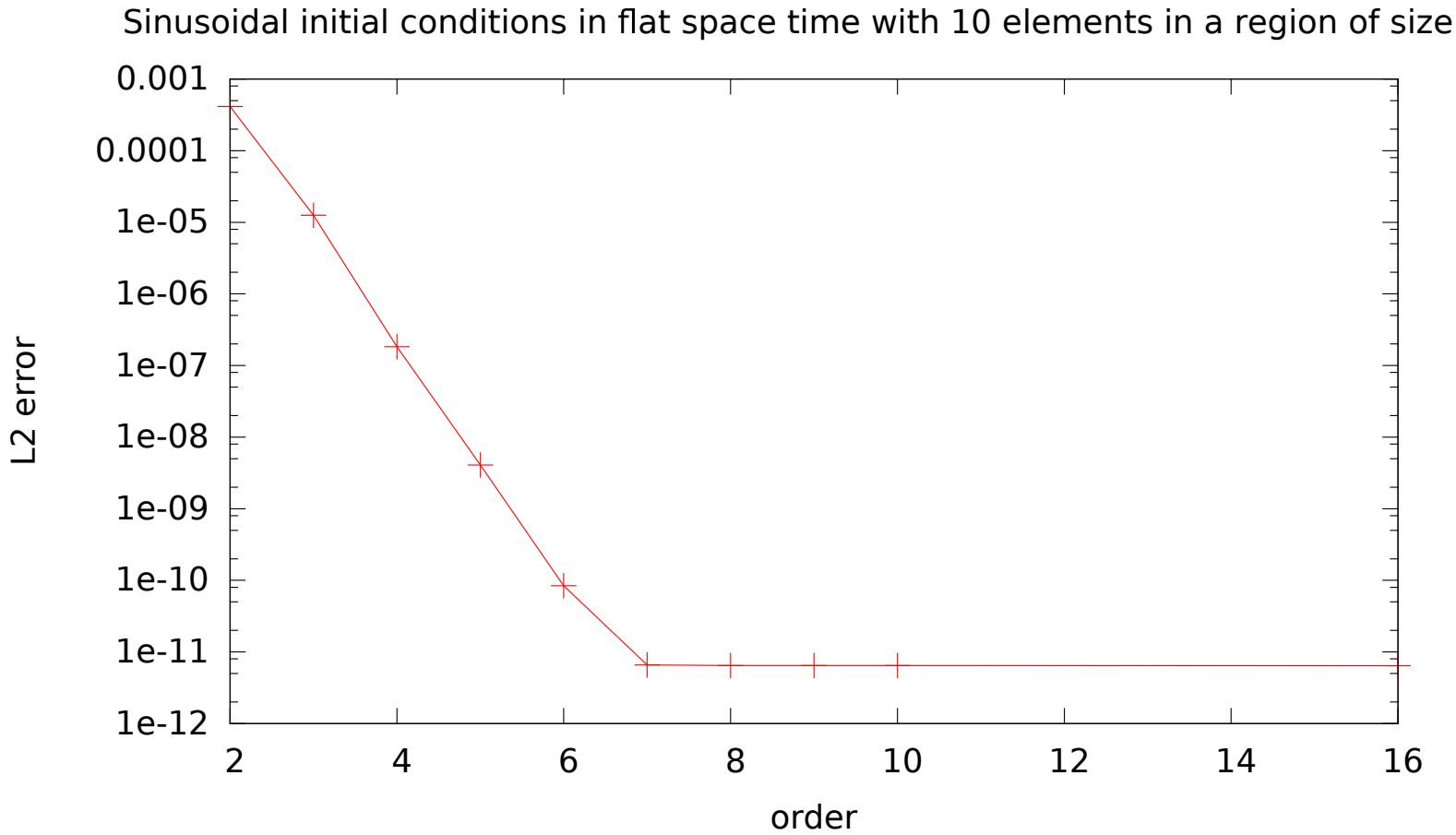


Figure: $L_2$ error converges exponentially until it hits roundoff noise with DG order for sinusiodal initial conditions with ten elements of size $h = 0.01$.

# Residuals to the l-mode fit

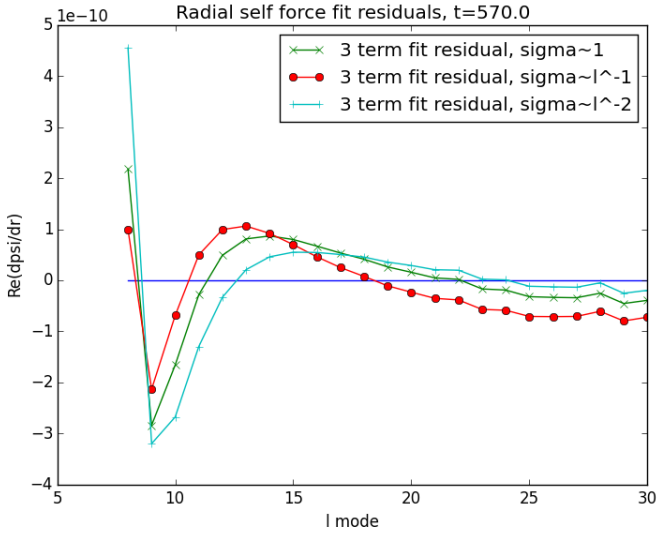


(a) $l_{min} = 8$

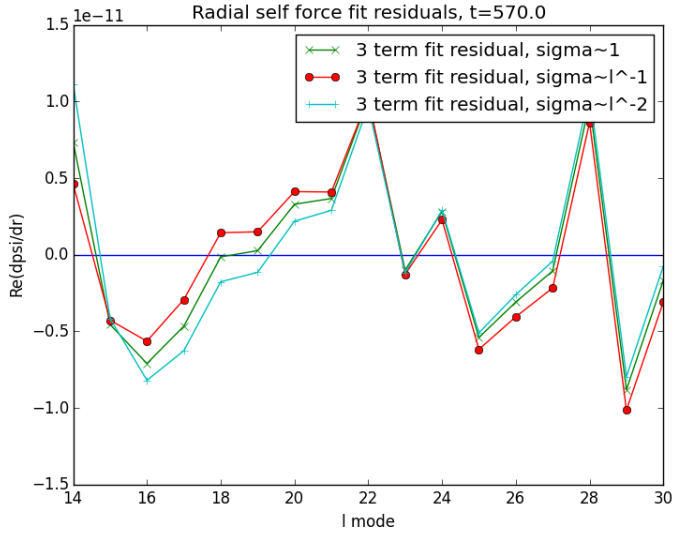


(b) $l_{min} = 14$

Figure: $l_{min} = 14$ is a better fit than $l_{min} = 8$ both because it is less systematically biased and because it has an amplitude an order of magnitude smaller. Both fits end at $l_{max} = 30$.

# Roundoff noise in $F_{inf}$ at high $l_{max}$

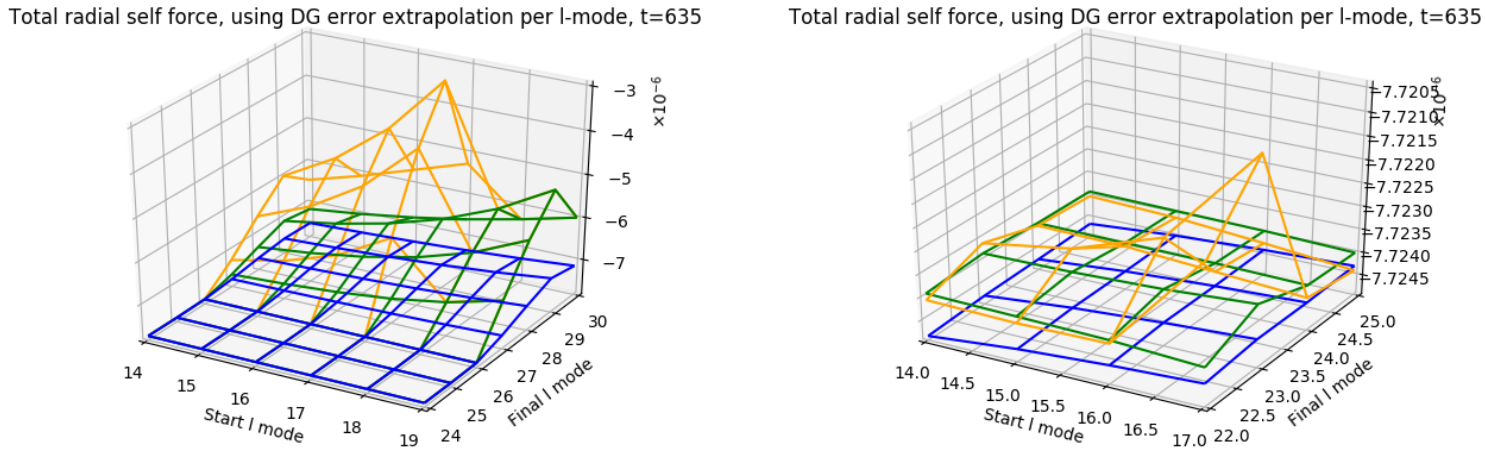


(a) Large range

(b) Small range

Figure: $l_{min} = 14$ and $l_{max} = 25$ appear to be good start and stop values. Roundoff noise is evident at higher l.

# Error due to l-mode selection, number of terms

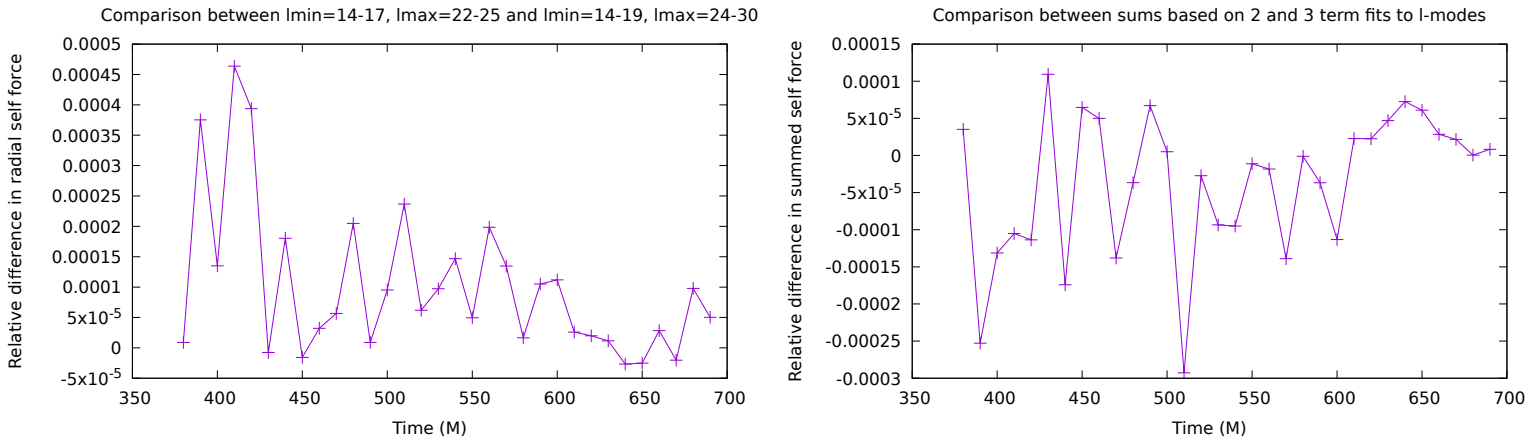


(a) large versus small range

(b) 2 versus 3 terms

Figure: Relative errors in both of these effects appear to be at the $10^{-4}$ level.